

Nirmatrelvir methyl *tert*-butyl ether solvate

Jared P. Smit,^{a*} Dale K. Purcell,^a David A. Engers,^a Pamela A. Smith,^a Haley C. Bauser^b and Adrian Radocea^b

^aImproved Pharma, LLC, 1281 Win Hentschel Blvd., West Lafayette, IN 47906, USA, and ^bVarda Space Industries, 225 S. Aviation Blvd., El Segundo, CA 90245, USA. *Correspondence e-mail: jared.smit@improvedpharma.com

Received 2 April 2026

Accepted 10 April 2026

Edited by J. Reibenspies, Texas A & M University, USA

Keywords: crystal structure; pharmaceutical; nirmatrelvir.

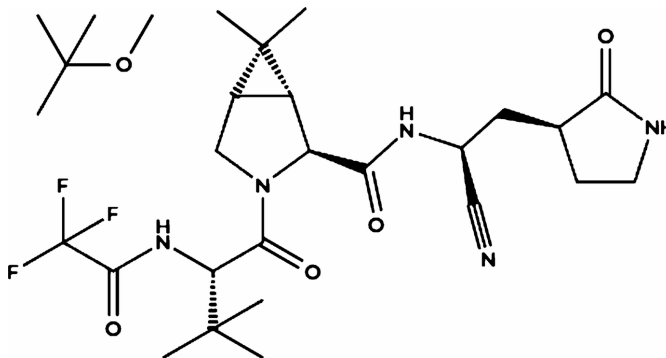
CCDC reference: 2545296

Supporting information: this article has supporting information at journals.iucr.org/e

The structure of nirmatrelvir MTBE solvate, $C_{23}H_{32}F_3N_5O_4 \cdot C_5H_{12}O$, at 150 K has monoclinic ($P2_1$) symmetry. The asymmetric unit contains one nirmatrelvir molecule and one methyl *tert*-butyl ether solvent molecule. The extended structure consists of $N-H \cdots O$ hydrogen bonds that create [010] chains. Crystals of the title compound were grown from various methyl *tert*-butyl ether–methanol solvent mixtures, with crystal morphology dependent upon the mixture ratio.

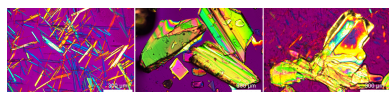
1. Chemical context

Nirmatrelvir (NTV) is an antiviral protease inhibitor developed by Pfizer, currently used in tandem with ritonavir and marketed as Paxlovid[®] for the treatment of Covid-19 (Halford, 2022; Lamb, 2022). Two enantiotropically related anhydrous polymorphs (designated Forms 1 and 4) of NTV have been well characterized, and the higher temperature stable form, Form 1, was selected for use in the drug product (Sadeghi *et al.*, 2024). A crystalline X-ray powder diffraction (XRPD) pattern for Form 2, a methyl *tert*-butyl ether (MTBE) solvate, was published in a US patent although the Form 2 crystal structure was not disclosed (Owens *et al.*, 2022). Form 2 is of interest as a key intermediate isolated in the purification process, enabling the subsequent generation of the stable, non-solvated Form 1 through recrystallization. The crystal structure of NTV Form 2, a mono-MTBE solvate, is reported in this work.



2. Structural commentary

The molecular structure of NTV is shown in Fig. 1. Nirmatrelvir Form 2 is a mono-MTBE solvate, crystallizing in space group $P2_1$, with an asymmetric unit consisting of one NTV molecule and one MTBE solvent molecule. The MTBE solvent molecule is disordered over two conformations that are approximate mirror images of each other, refining to 69%



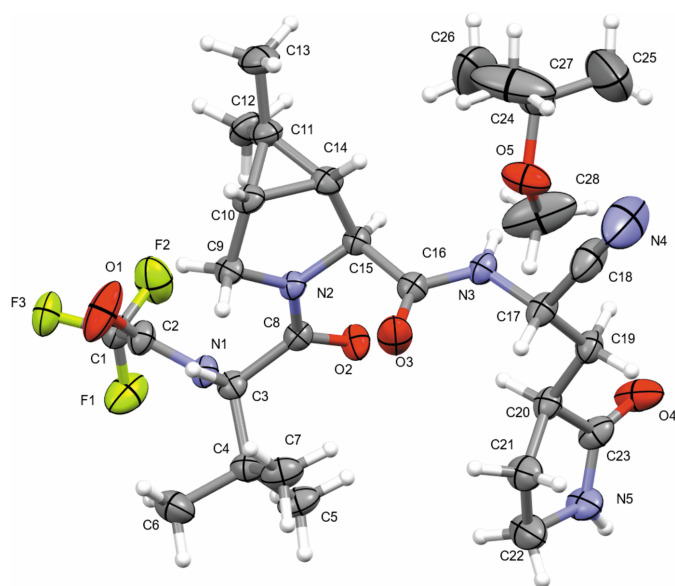


Figure 1
The title molecule with displacement ellipsoids drawn at the 50% probability level. Solvent disorder is not shown for clarity.

in the predominant orientation. The absolute structure was determined from the data and the NTV molecule was found to bond in the *S, S, R, S, S*, and *S* configuration at C3, C10, C14, C15, C17, and C20 respectively.

3. Supramolecular features

Nirmatrelvir contains three secondary amide moieties that are available for hydrogen-bond donation. The pyrrolidone amide forms a hydrogen bond to the pyrrolidine amide carbonyl and accepts a hydrogen bond from the trifluoroacetyl amide from an adjacent molecule, creating hydrogen bonded chains propagating along the *b*-axis direction, shown in Fig. 2. The pyrimidine NH grouping forms a hydrogen bond to the oxygen atom of the MTBE, but this supramolecular feature does not

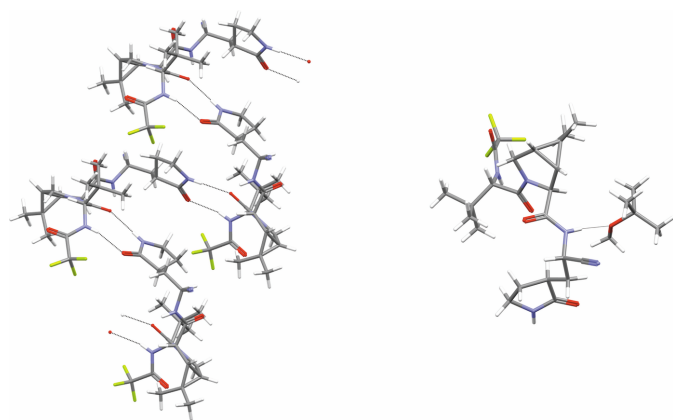


Figure 2
One-dimensional hydrogen-bonded chain of nirmatrelvir molecules (left) and NTV hydrogen bonded to MTBE (right).

Table 1
Hydrogen-bond geometry (Å, °).

<i>D</i> –H··· <i>A</i>	<i>D</i> –H	H··· <i>A</i>	<i>D</i> ··· <i>A</i>	<i>D</i> –H··· <i>A</i>
N1–H1···O4 ⁱ	0.80 (3)	2.06 (3)	2.837 (2)	165 (4)
N3–H3···O5	0.87 (3)	1.99 (3)	2.848 (4)	170 (2)
N3–H3···O5A	0.87 (3)	1.95 (3)	2.795 (10)	163 (3)
N5–H5···O2 ⁱⁱ	0.85 (3)	2.00 (3)	2.845 (2)	176 (3)

Symmetry codes: (i) $-x + 1, y + \frac{1}{2}, -z + 1$; (ii) $-x + 1, y - \frac{1}{2}, -z + 1$.

contribute to the dimensionality. Geometric details of hydrogen bonds are given in Table 1.

4. Database survey

Two anhydrous polymorphs are in the Cambridge Structural Database (CSD, version 6.01, update 1, February 2026; Groom *et al.*, 2016), refcodes ZIVMEA through ZIVMEA10 (Sadeghi *et al.*, 2024; Jiang *et al.*, 2023).. The two forms are enantiotropic polymorphs, both crystallizing in space group $P2_12_12_1$, and the molecular packing is similar enough that the two forms can undergo a first order solid-state single crystal-to-single crystal phase transition (Shi *et al.*, 2025). The pyrrolidone amide forms and accepts hydrogen bonds to and from the same amide oxygen moiety on two different adjacent molecules rather than the hydrogen bonding to the pyrrolidine amide and from the trifluoroacetyl amide on one adjacent molecule in the framework of the title solvate.

Isostructural ethanol and isopropanol solvates (refcodes AMEPOB and AMESOE) have also been reported (Li *et al.*, 2026). These solvates have three NTV molecules in the asymmetric unit, each forming different hydrogen bonds. The pyrrolidone amide moiety on one of the three unique molecules forms the same hydrogen bonds as in the structure of the MTBE solvate.

5. Synthesis and crystallization

Nirmatrelvir was obtained from ChemShuttle and used without purification. Single crystals were obtained from MTBE and from solutions of 94 to 99% (*v/v*) MTBE in methanol. The solid (0.02 g) was dissolved in each MTBE solution. After standing at room temperature overnight, a solid precipitate was observed. Solubilities of NTV in each solution were determined gravimetrically from supernatant filtered through a 0.2 mm PTFE membrane into clean prepared vials. The measured solubilities ranged from 0.7 mg ml⁻¹ in MTBE to 6.5 mg ml⁻¹ in 94% (*v/v*) MTBE–methanol

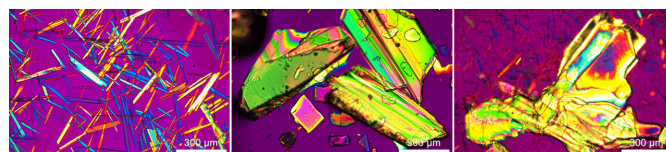


Figure 3
Morphology of NTV MTBE solvate crystals at MTBE:methanol ratios of 99:1, 96:4, and 95:5 (left to right)

solution. After standing at room temperature for an extended time (18 months), crystals suitable for single crystal X-ray diffraction (SCXRD) were discovered and isolated. The apparent morphology of the crystals varied with solution composition, with finer blades and needle-shaped crystals obtained at 99% (v/v) MTBE and larger block-shaped and prismatic crystals obtained as methanol concentration increased, 95–96% (v/v) MTBE, shown in polarized light microscopy images (Fig. 3).

Polarized light microscopy was conducted using an Olympus Series BX51TRF (Olympus America Inc., Melville, NY) equipped with 12 V/100 W transmission and reflection illumination, an achromat 0.9 NA polarized light condenser, Olympus Series MPlanFL N objectives: 50X/0.75 NA BDP, 20X/0.40 NA BDP, 10X/0.25 NA BDP, 5X/0.15 NA BDP, an intermediate tube with variable position analyzer and compensator, a trinocular viewing head with a Lumenera Series Infinity 3-3URC (Teledyne Lumenera, Ottawa, Ontario, Canada) digital camera. Image capture and image processing using Image-Pro® version 10.0.11 Build 7240 (Date: 01-April-2020).

A small portion of the sample was pipetted into the well of a scrupulously cleaned depression microscope slide and a No. 1½ cover glass was placed over the sample, which was sealed using grease to prevent fast of the volatile solvent.

The relatively larger amount of the more polar methanol in MTBE increased the solubility and therefore decreased the nucleation rate, leading to fewer, but larger, crystals. Face indexing using *CrysAlis PRO* (Rigaku OD, 2026) indicates that the needles are growing faster along the [010] direction, consistent with the direction of hydrogen bonding and therefore the presence of the hydrogen-bond donating methanol slows that process (McArdle & Erxleben, 2024). Crystals from each solution were indexed with unit-cell parameters matching the crystal structure of the MTBE solvate. The XRPD pattern calculated from the crystal structure is consistent with the powder pattern previously published (Owens *et al.*, 2022).

6. Refinement

Crystal data, data collection and structure refinement details are summarized in Table 2. Hydrogen atoms residing on nitrogen were refined independently. Hydrogen atoms residing on carbon were included in the refinement using the appropriate riding models. The MTBE molecule is disordered over two orientations that are related through a pseudo-inversion, refining to 69% in the predominant orientation, and modeled using restraints to the anisotropic displacement parameters (SIMU/DELU).

Acknowledgements

The authors declare the following competing financial interest(s): H. C. Bauser and A. Radocea are employees of Varda Space Industries and may own Varda Space Industries stock.

Table 2

Experimental details.

Crystal data	
Chemical formula	C ₂₃ H ₃₂ F ₃ N ₅ O ₄ ·C ₅ H ₁₂ O
<i>M_r</i>	587.68
Crystal system, space group	Monoclinic, <i>P</i> 2 ₁
Temperature (K)	150
<i>a</i> , <i>b</i> , <i>c</i> (Å)	12.7655 (1), 9.2588 (1), 14.3951 (1)
β (°)	103.208 (1)
<i>V</i> (Å ³)	1656.40 (3)
<i>Z</i>	2
Radiation type	Cu <i>K</i> α
μ (mm ⁻¹)	0.78
Crystal size (mm)	0.35 × 0.24 × 0.12
Data collection	
Diffractometer	XtaLAB Synergy, Single source at home/near, HyPix-Bantam
Absorption correction	Multi-scan (<i>CrysAlis PRO</i> ; Rigaku OD, 2026)
<i>T_{min}</i> , <i>T_{max}</i>	0.691, 1.000
No. of measured, independent and observed [<i>I</i> > 2 σ (<i>I</i>)] reflections	31765, 5959, 5890
<i>R_{int}</i>	0.023
($\sin \theta/\lambda$) _{max} (Å ⁻¹)	0.604
Refinement	
$R[F^2 > 2\sigma(F^2)]$, $wR(F^2)$, <i>S</i>	0.035, 0.094, 1.03
No. of reflections	5959
No. of parameters	442
No. of restraints	46
H-atom treatment	H atoms treated by a mixture of independent and constrained refinement
$\Delta\rho_{\max}$, $\Delta\rho_{\min}$ (e Å ⁻³)	0.29, -0.20
Absolute structure	Flack <i>x</i> determined using 2630 quotients [(<i>I</i> ⁺) - (<i>I</i> ⁻)]/[(<i>I</i> ⁺) + (<i>I</i> ⁻)] (Parsons <i>et al.</i> , 2013)
Absolute structure parameter	-0.03 (3)

Computer programs: *CrysAlis PRO* (Rigaku OD, 2026), *SHELXT* (Sheldrick, 2015a), *SHELXL2018/3* (Sheldrick, 2015b) and *OLEX2* (Dolomanov *et al.*, 2009).

References

- Dolomanov, O. V., Bourhis, L. J., Gildea, R. J., Howard, J. A. K. & Puschmann, H. (2009). *J. Appl. Cryst.* **42**, 339–341.
- Groom, C. R., Bruno, I. J., Lightfoot, M. P. & Ward, S. C. (2016). *Acta Cryst. B* **72**, 171–179.
- Halford, B. (2022). *ACS Cent. Sci.* **8**, 405–407.
- Jiang, B., Li, G., Yu, J., Xu, X., Pan, H., Zhao, C., Zhong, J. & Zhang, F. (2023). *React. Chem. Eng.* **8**, 1747–1759.
- Lamb, Y. N. (2022). *Drugs* **82**, 585–591.
- Li, G., Sun, W., Yang, J., Shan, H., Pan, H., Zhang, F., Zuo, L. & Zhong, J. (2026). *J. Mol. Struct.* **1350**, 144145.
- McArdle, P. & Erxleben, A. (2024). *CrystEngComm* **26**, 416–430.
- Owens, D. R., Pettersson, M. Y., Reese, M. R., Sammons, M. F., Tuttle, J. B., Verhoest, P. R., Wei, L., Yang, Q. & Yang, X. (2022). US Patent Number 11,351,149 B2, US Patent and Trademark Office.
- Parsons, S., Flack, H. D. & Wagner, T. (2013). *Acta Cryst. B* **69**, 249–259.
- Rigaku OD, (2026). *CrysAlis PRO* Software System. Rigaku Corporation, Wroclaw, Poland
- Sadeghi, M. S., Guo, R., Bellucci, M. A., Quino, J., Buckle, E. L., Nisbet, M. L., Yang, Z., Greenwell, C., Gorka, D. E., Pickard Iv, F. C., Wood, G. P. F., Sun, G., Wen, S.-H., Krzyzaniak, J. F., Meenan, P. A., Hancock, B. C. & Yang, X. H. (2024). *Mol. Pharm.* **21**, 3800–3814.
- Sheldrick, G. M. (2015a). *Acta Cryst. A* **71**, 3–8.
- Sheldrick, G. M. (2015b). *Acta Cryst. C* **71**, 3–8.
- Shi, D., Liu, J., Liu, S., Wang, Y., Yu, K. & Hu, X. (2025). *CrystEngComm* **27**, 6009–6018.

supporting information

Acta Cryst. (2026). E82, 477-479 [https://doi.org/10.1107/S2056989026003816]

Nirmatrelvir methyl *tert*-butyl ether solvate

Jared P. Smit, Dale K. Purcell, David A. Engers, Pamela A. Smith, Haley C. Bauser and Adrian Radocea

Computing details

(1*R*,2*S*,5*S*)-*N*-[(1*S*)-1-Cyano-2-[(3*S*)-2-oxopyrrolidin-3-yl]ethyl]-3-[(2*S*)-3,3-dimethyl-2-[(2,2-trifluoroacetyl)amino]butanoyl]-6,6-dimethyl-3-azabicyclohexane-2-carboxamide methyl *tert*-butyl ether monosolvate

Crystal data

C₂₃H₃₂F₃N₅O₄·C₅H₁₂O

M_r = 587.68

Monoclinic, *P*2₁

a = 12.7655 (1) Å

b = 9.2588 (1) Å

c = 14.3951 (1) Å

β = 103.208 (1)°

V = 1656.40 (3) Å³

Z = 2

F(000) = 628

D_x = 1.178 Mg m⁻³

Cu *Kα* radiation, λ = 1.54184 Å

Cell parameters from 28535 reflections

θ = 3.2–68.6°

μ = 0.78 mm⁻¹

T = 150 K

Block, colourless

0.35 × 0.24 × 0.12 mm

Data collection

XtaLAB Synergy, Single source at home/near,

HyPix-Bantam

diffractometer

Radiation source: micro-focus sealed X-ray

tube, PhotonJet (Cu) X-ray Source

Mirror monochromator

Detector resolution: 10.0000 pixels mm⁻¹

ω scans

Absorption correction: multi-scan

(CrysAlisPro; Rigaku OD, 2026)

T_{min} = 0.691, *T_{max}* = 1.000

31765 measured reflections

5959 independent reflections

5890 reflections with *I* > 2σ(*I*)

R_{int} = 0.023

θ_{max} = 68.7°, θ_{min} = 3.2°

h = -15→15

k = -11→11

l = -17→17

Refinement

Refinement on *F*²

Least-squares matrix: full

R[[*F*² > 2σ(*F*²)]] = 0.035

wR(*F*²) = 0.094

S = 1.03

5959 reflections

442 parameters

46 restraints

Primary atom site location: dual

Hydrogen site location: mixed

H atoms treated by a mixture of independent and constrained refinement

w = 1/[σ²(*F_o*²) + (0.062*P*)² + 0.2608*P*]

where *P* = (*F_o*² + 2*F_c*²)/3

(Δ/σ)_{max} = 0.001

Δρ_{max} = 0.29 e Å⁻³

Δρ_{min} = -0.20 e Å⁻³

Absolute structure: Flack *x* determined using 2630 quotients [(*F*⁺)-(*F*)]/[(*F*⁺)+(*F*)] (Parsons *et al.*, 2013)

Absolute structure parameter: -0.03 (3)

Special details

Geometry. All esds (except the esd in the dihedral angle between two l.s. planes) are estimated using the full covariance matrix. The cell esds are taken into account individually in the estimation of esds in distances, angles and torsion angles; correlations between esds in cell parameters are only used when they are defined by crystal symmetry. An approximate (isotropic) treatment of cell esds is used for estimating esds involving l.s. planes.

Fractional atomic coordinates and isotropic or equivalent isotropic displacement parameters (\AA^2)

	<i>x</i>	<i>y</i>	<i>z</i>	$U_{\text{iso}}^*/U_{\text{eq}}$	Occ. (<1)
F3	0.71689 (12)	0.98226 (17)	0.18387 (10)	0.0502 (4)	
O2	0.42888 (11)	0.49248 (18)	0.29537 (9)	0.0346 (3)	
F2	0.63537 (16)	0.9574 (2)	0.29654 (13)	0.0622 (5)	
F1	0.77491 (12)	0.82994 (19)	0.29599 (12)	0.0575 (4)	
N2	0.34108 (12)	0.54106 (18)	0.14552 (11)	0.0260 (3)	
N1	0.60011 (13)	0.6527 (2)	0.22920 (12)	0.0291 (4)	
O3	0.24679 (16)	0.2686 (2)	0.13660 (13)	0.0480 (4)	
O4	0.32501 (18)	0.1791 (2)	0.57021 (11)	0.0584 (6)	
N3	0.16245 (13)	0.3324 (2)	0.25251 (12)	0.0308 (4)	
N5	0.45298 (16)	0.0532 (3)	0.51601 (13)	0.0431 (5)	
O1	0.5744 (2)	0.7964 (3)	0.09820 (14)	0.0756 (8)	
C1	0.68689 (17)	0.8859 (3)	0.23966 (15)	0.0358 (5)	
C8	0.43156 (15)	0.5203 (2)	0.21144 (13)	0.0264 (4)	
C15	0.23765 (14)	0.5218 (2)	0.17219 (13)	0.0265 (4)	
H15	0.236566	0.576525	0.231853	0.032*	
C16	0.21747 (15)	0.3610 (2)	0.18512 (14)	0.0300 (4)	
C2	0.61382 (17)	0.7711 (3)	0.18146 (14)	0.0341 (4)	
C3	0.53816 (14)	0.5313 (2)	0.18022 (13)	0.0288 (4)	
H3A	0.520209	0.554521	0.110540	0.035*	
C23	0.36464 (19)	0.1326 (3)	0.50598 (15)	0.0377 (5)	
C10	0.21163 (16)	0.6146 (2)	0.00894 (14)	0.0324 (4)	
H10	0.174056	0.589426	-0.057936	0.039*	
C14	0.15510 (15)	0.5825 (2)	0.08827 (14)	0.0316 (4)	
H14	0.082198	0.536855	0.071303	0.038*	
C17	0.14115 (18)	0.1852 (3)	0.27582 (15)	0.0363 (5)	
H17	0.169676	0.119004	0.232567	0.044*	
C11	0.16674 (18)	0.7362 (3)	0.05803 (15)	0.0366 (5)	
C9	0.32856 (16)	0.5740 (3)	0.04271 (13)	0.0311 (4)	
H9A	0.346067	0.488590	0.007773	0.037*	
H9B	0.375806	0.655132	0.033691	0.037*	
C20	0.31739 (16)	0.1561 (3)	0.39984 (13)	0.0333 (4)	
H20	0.338981	0.253910	0.381412	0.040*	
C19	0.19543 (17)	0.1480 (3)	0.37928 (15)	0.0356 (5)	
H19A	0.169260	0.215436	0.422334	0.043*	
H19B	0.174017	0.049149	0.393515	0.043*	
O5	0.1325 (3)	0.5375 (4)	0.3916 (2)	0.0557 (10)	0.687 (8)
C4	0.60242 (17)	0.3874 (3)	0.19259 (15)	0.0355 (5)	
C21	0.3745 (2)	0.0415 (3)	0.35336 (15)	0.0457 (6)	
H21A	0.386753	0.075998	0.291617	0.055*	

H21B	0.332176	-0.049036	0.342658	0.055*	
C12	0.2382 (2)	0.8424 (3)	0.12260 (18)	0.0461 (5)	
H12A	0.307656	0.796793	0.150239	0.069*	
H12B	0.203839	0.871835	0.173883	0.069*	
H12C	0.249686	0.927433	0.085634	0.069*	
C5	0.6507 (2)	0.3496 (3)	0.29742 (17)	0.0448 (6)	
H5A	0.696781	0.429029	0.327825	0.067*	
H5B	0.693608	0.261189	0.300766	0.067*	
H5C	0.592597	0.334485	0.330615	0.067*	
C7	0.5265 (2)	0.2675 (3)	0.14520 (18)	0.0443 (5)	
H7A	0.469853	0.253609	0.180198	0.066*	
H7B	0.567102	0.177540	0.145900	0.066*	
H7C	0.493925	0.294566	0.079088	0.066*	
C22	0.4812 (2)	0.0190 (4)	0.42612 (18)	0.0550 (7)	
H22A	0.506473	-0.081976	0.425368	0.066*	
H22B	0.537516	0.084957	0.413796	0.066*	
C13	0.0639 (2)	0.8043 (4)	0.0006 (2)	0.0557 (7)	
H13A	0.081874	0.878817	-0.041587	0.084*	
H13B	0.024111	0.848199	0.044097	0.084*	
H13C	0.019303	0.729924	-0.037838	0.084*	
C6	0.6935 (2)	0.4043 (3)	0.1404 (2)	0.0514 (6)	
H6A	0.662914	0.420029	0.072286	0.077*	
H6B	0.737522	0.316514	0.148864	0.077*	
H6C	0.738318	0.487166	0.166663	0.077*	
C18	0.0234 (2)	0.1619 (3)	0.2606 (2)	0.0582 (8)	
N4	-0.0664 (2)	0.1441 (4)	0.2507 (3)	0.0961 (13)	
C27	0.0365 (3)	0.6271 (5)	0.3776 (3)	0.0502 (12)	0.687 (8)
C28	0.2129 (10)	0.5420 (14)	0.4736 (7)	0.101 (4)	0.687 (8)
H28A	0.269746	0.473453	0.468243	0.151*	0.687 (8)
H28B	0.243009	0.639743	0.482490	0.151*	0.687 (8)
H28C	0.183275	0.516023	0.528416	0.151*	0.687 (8)
C24	-0.0276 (6)	0.5901 (14)	0.2767 (7)	0.133 (5)	0.687 (8)
H24A	0.017885	0.604487	0.231128	0.199*	0.687 (8)
H24B	-0.050962	0.489079	0.274766	0.199*	0.687 (8)
H24C	-0.090841	0.653078	0.259808	0.199*	0.687 (8)
C26	0.0834 (11)	0.7670 (11)	0.3672 (11)	0.183 (7)	0.687 (8)
H26A	0.120388	0.763557	0.314619	0.275*	0.687 (8)
H26B	0.026426	0.840144	0.353478	0.275*	0.687 (8)
H26C	0.135088	0.792067	0.426510	0.275*	0.687 (8)
C25	-0.0220 (11)	0.6102 (18)	0.4520 (11)	0.231 (10)	0.687 (8)
H25A	-0.049249	0.511175	0.451164	0.347*	0.687 (8)
H25B	0.026171	0.630006	0.514173	0.347*	0.687 (8)
H25C	-0.082490	0.678083	0.441141	0.347*	0.687 (8)
H3	0.147 (2)	0.399 (3)	0.290 (2)	0.037 (7)*	
H5	0.491 (2)	0.035 (4)	0.571 (2)	0.048 (8)*	
H1	0.625 (3)	0.645 (4)	0.285 (2)	0.050 (8)*	
C28A	-0.0441 (7)	0.5301 (14)	0.3463 (16)	0.086 (5)	0.313 (8)
H28D	-0.076611	0.463036	0.295219	0.129*	0.313 (8)

H28E	-0.068231	0.505978	0.404360	0.129*	0.313 (8)
H28F	-0.065948	0.629095	0.326818	0.129*	0.313 (8)
O5A	0.0714 (8)	0.5189 (11)	0.3649 (7)	0.075 (3)	0.313 (8)
C27A	0.1104 (9)	0.6173 (10)	0.4379 (7)	0.061 (3)	0.313 (8)
C25A	0.0502 (12)	0.7738 (16)	0.414 (2)	0.165 (14)	0.313 (8)
H25D	0.078353	0.841867	0.465413	0.248*	0.313 (8)
H25E	0.063707	0.811400	0.353747	0.248*	0.313 (8)
H25F	-0.027408	0.761711	0.407048	0.248*	0.313 (8)
C24A	0.2273 (17)	0.591 (3)	0.465 (2)	0.133 (15)	0.313 (8)
H24D	0.260701	0.656770	0.516101	0.199*	0.313 (8)
H24E	0.240780	0.490800	0.486222	0.199*	0.313 (8)
H24F	0.258158	0.607410	0.409066	0.199*	0.313 (8)
C26A	0.0671 (15)	0.583 (4)	0.5248 (13)	0.184 (15)	0.313 (8)
H26D	0.095278	0.653228	0.575311	0.275*	0.313 (8)
H26E	-0.011687	0.588288	0.507957	0.275*	0.313 (8)
H26F	0.089540	0.485615	0.547460	0.275*	0.313 (8)

Atomic displacement parameters (Å²)

	U^{11}	U^{22}	U^{33}	U^{12}	U^{13}	U^{23}
F3	0.0568 (8)	0.0476 (9)	0.0466 (7)	-0.0173 (7)	0.0125 (6)	0.0103 (6)
O2	0.0304 (7)	0.0502 (9)	0.0207 (6)	-0.0057 (6)	0.0009 (5)	0.0028 (6)
F2	0.0774 (11)	0.0554 (10)	0.0626 (10)	-0.0134 (8)	0.0344 (9)	-0.0182 (8)
F1	0.0467 (7)	0.0512 (9)	0.0614 (9)	-0.0119 (7)	-0.0154 (7)	0.0109 (7)
N2	0.0268 (7)	0.0292 (9)	0.0209 (7)	-0.0007 (6)	0.0029 (6)	0.0007 (6)
N1	0.0291 (8)	0.0358 (10)	0.0202 (8)	-0.0041 (7)	0.0011 (6)	0.0021 (7)
O3	0.0662 (11)	0.0326 (9)	0.0515 (10)	-0.0062 (8)	0.0268 (8)	-0.0101 (7)
O4	0.0767 (12)	0.0669 (13)	0.0258 (8)	0.0359 (11)	-0.0006 (7)	-0.0044 (8)
N3	0.0334 (8)	0.0299 (9)	0.0268 (8)	-0.0039 (7)	0.0023 (7)	0.0018 (7)
N5	0.0417 (10)	0.0575 (13)	0.0252 (9)	0.0101 (9)	-0.0026 (7)	0.0043 (8)
O1	0.1116 (18)	0.0650 (15)	0.0349 (10)	-0.0384 (13)	-0.0147 (10)	0.0176 (9)
C1	0.0381 (11)	0.0349 (12)	0.0335 (10)	-0.0039 (9)	0.0066 (9)	0.0045 (9)
C8	0.0288 (9)	0.0254 (9)	0.0227 (8)	-0.0029 (7)	0.0013 (7)	-0.0021 (7)
C15	0.0264 (8)	0.0279 (10)	0.0238 (8)	-0.0017 (7)	0.0029 (7)	-0.0008 (7)
C16	0.0278 (9)	0.0318 (11)	0.0278 (9)	-0.0034 (8)	0.0007 (7)	-0.0014 (8)
C2	0.0364 (10)	0.0378 (12)	0.0263 (10)	-0.0043 (9)	0.0032 (8)	0.0045 (9)
C3	0.0266 (9)	0.0353 (11)	0.0214 (8)	-0.0001 (8)	-0.0007 (7)	0.0001 (7)
C23	0.0469 (12)	0.0357 (12)	0.0250 (10)	0.0020 (9)	-0.0030 (8)	-0.0007 (8)
C10	0.0328 (10)	0.0368 (11)	0.0242 (9)	0.0046 (8)	-0.0004 (7)	0.0015 (8)
C14	0.0264 (9)	0.0375 (11)	0.0283 (9)	0.0014 (8)	0.0011 (7)	-0.0005 (8)
C17	0.0364 (10)	0.0347 (12)	0.0325 (10)	-0.0079 (9)	-0.0031 (8)	0.0057 (9)
C11	0.0376 (11)	0.0371 (12)	0.0343 (10)	0.0108 (9)	0.0067 (8)	0.0058 (9)
C9	0.0318 (9)	0.0399 (12)	0.0198 (9)	0.0046 (8)	0.0022 (7)	0.0028 (8)
C20	0.0352 (10)	0.0374 (11)	0.0242 (9)	-0.0033 (9)	0.0005 (7)	0.0047 (8)
C19	0.0366 (10)	0.0381 (12)	0.0308 (10)	-0.0027 (9)	0.0050 (8)	0.0089 (9)
O5	0.0424 (18)	0.070 (2)	0.0494 (17)	0.0150 (17)	-0.0005 (14)	-0.0184 (15)
C4	0.0354 (10)	0.0379 (12)	0.0302 (10)	0.0055 (9)	0.0014 (8)	-0.0028 (9)
C21	0.0481 (12)	0.0608 (16)	0.0262 (10)	0.0103 (11)	0.0046 (9)	0.0014 (10)

C12	0.0617 (14)	0.0274 (12)	0.0499 (13)	0.0038 (10)	0.0144 (11)	0.0003 (10)
C5	0.0483 (12)	0.0401 (13)	0.0380 (12)	0.0101 (10)	-0.0064 (10)	0.0011 (10)
C7	0.0486 (13)	0.0352 (12)	0.0434 (13)	0.0050 (10)	-0.0013 (10)	-0.0083 (10)
C22	0.0502 (13)	0.080 (2)	0.0346 (11)	0.0178 (14)	0.0094 (10)	0.0104 (12)
C13	0.0519 (14)	0.0627 (19)	0.0515 (15)	0.0282 (13)	0.0093 (11)	0.0170 (13)
C6	0.0418 (12)	0.0605 (17)	0.0536 (15)	0.0105 (12)	0.0144 (11)	-0.0055 (13)
C18	0.0457 (15)	0.0526 (17)	0.0647 (17)	-0.0178 (12)	-0.0117 (12)	0.0222 (14)
N4	0.0440 (14)	0.094 (3)	0.132 (3)	-0.0278 (15)	-0.0163 (16)	0.043 (2)
C27	0.045 (2)	0.046 (2)	0.064 (3)	0.0086 (17)	0.022 (2)	-0.0032 (18)
C28	0.143 (8)	0.063 (7)	0.066 (4)	0.032 (5)	-0.040 (4)	-0.036 (4)
C24	0.078 (4)	0.185 (11)	0.111 (6)	0.072 (6)	-0.030 (4)	-0.060 (7)
C26	0.220 (13)	0.068 (6)	0.327 (18)	0.028 (7)	0.198 (14)	0.059 (8)
C25	0.205 (13)	0.29 (2)	0.264 (17)	0.148 (14)	0.192 (14)	0.172 (16)
C28A	0.027 (4)	0.057 (7)	0.161 (16)	0.006 (4)	-0.005 (6)	0.013 (8)
O5A	0.056 (5)	0.083 (6)	0.083 (6)	0.017 (5)	0.011 (4)	-0.026 (5)
C27A	0.091 (8)	0.041 (5)	0.060 (6)	-0.005 (5)	0.036 (6)	-0.005 (4)
C25A	0.061 (8)	0.054 (9)	0.34 (3)	0.016 (7)	-0.039 (14)	-0.090 (15)
C24A	0.100 (13)	0.08 (2)	0.16 (2)	0.034 (12)	-0.077 (14)	-0.074 (16)
C26A	0.095 (12)	0.36 (4)	0.116 (14)	-0.01 (2)	0.065 (11)	-0.06 (2)

Geometric parameters (Å, °)

F3—C1	1.314 (3)	C10—C9	1.508 (3)
O2—C8	1.243 (2)	C14—C11	1.506 (3)
F2—C1	1.337 (3)	C17—C19	1.531 (3)
F1—C1	1.331 (3)	C17—C18	1.484 (3)
N2—C8	1.331 (2)	C11—C12	1.508 (3)
N2—C15	1.468 (2)	C11—C13	1.520 (3)
N2—C9	1.484 (2)	C20—C19	1.519 (3)
N1—C2	1.327 (3)	C20—C21	1.525 (3)
N1—C3	1.460 (3)	O5—C27	1.456 (5)
O3—C16	1.216 (3)	O5—C28	1.376 (10)
O4—C23	1.229 (3)	C4—C5	1.535 (3)
N3—C16	1.348 (3)	C4—C7	1.528 (3)
N3—C17	1.444 (3)	C4—C6	1.529 (3)
N5—C23	1.326 (3)	C21—C22	1.531 (3)
N5—C22	1.455 (3)	C18—N4	1.135 (4)
O1—C2	1.212 (3)	C27—C24	1.534 (8)
C1—C2	1.531 (3)	C27—C26	1.449 (10)
C8—C3	1.531 (3)	C27—C25	1.448 (9)
C15—C16	1.529 (3)	C28A—O5A	1.440 (12)
C15—C14	1.518 (3)	O5A—C27A	1.394 (13)
C3—C4	1.553 (3)	C27A—C25A	1.641 (16)
C23—C20	1.525 (3)	C27A—C24A	1.47 (2)
C10—C14	1.513 (3)	C27A—C26A	1.513 (17)
C10—C11	1.510 (3)		
C8—N2—C15	118.82 (16)	N3—C17—C18	110.0 (2)

C8—N2—C9	128.26 (16)	C18—C17—C19	109.19 (19)
C15—N2—C9	112.80 (15)	C10—C11—C13	115.3 (2)
C2—N1—C3	120.48 (17)	C14—C11—C10	60.22 (14)
C16—N3—C17	120.65 (19)	C14—C11—C12	121.58 (19)
C23—N5—C22	113.62 (19)	C14—C11—C13	114.8 (2)
F3—C1—F2	106.9 (2)	C12—C11—C10	122.23 (19)
F3—C1—F1	108.25 (18)	C12—C11—C13	113.0 (2)
F3—C1—C2	111.28 (17)	N2—C9—C10	104.24 (15)
F2—C1—C2	110.81 (19)	C23—C20—C21	102.78 (18)
F1—C1—F2	106.53 (19)	C19—C20—C23	109.96 (17)
F1—C1—C2	112.8 (2)	C19—C20—C21	116.8 (2)
O2—C8—N2	120.71 (17)	C20—C19—C17	113.22 (17)
O2—C8—C3	121.51 (17)	C28—O5—C27	122.8 (6)
N2—C8—C3	117.78 (16)	C5—C4—C3	113.04 (18)
N2—C15—C16	109.67 (15)	C7—C4—C3	107.91 (17)
N2—C15—C14	104.44 (15)	C7—C4—C5	110.2 (2)
C14—C15—C16	110.58 (16)	C7—C4—C6	109.3 (2)
O3—C16—N3	123.7 (2)	C6—C4—C3	107.3 (2)
O3—C16—C15	122.15 (19)	C6—C4—C5	109.06 (19)
N3—C16—C15	114.15 (18)	C20—C21—C22	103.54 (19)
N1—C2—C1	115.23 (17)	N5—C22—C21	102.51 (19)
O1—C2—N1	126.7 (2)	N4—C18—C17	178.8 (4)
O1—C2—C1	118.1 (2)	O5—C27—C24	104.8 (4)
N1—C3—C8	109.22 (16)	C26—C27—O5	99.8 (6)
N1—C3—C4	113.04 (16)	C26—C27—C24	104.2 (9)
C8—C3—C4	113.02 (17)	C25—C27—O5	113.3 (6)
O4—C23—N5	126.7 (2)	C25—C27—C24	115.0 (9)
O4—C23—C20	124.6 (2)	C25—C27—C26	117.9 (10)
N5—C23—C20	108.67 (19)	C27A—O5A—C28A	105.5 (10)
C11—C10—C14	59.74 (14)	O5A—C27A—C25A	110.3 (10)
C9—C10—C14	108.39 (16)	O5A—C27A—C24A	104.7 (12)
C9—C10—C11	119.22 (18)	O5A—C27A—C26A	110.6 (13)
C10—C14—C15	108.01 (15)	C24A—C27A—C25A	126.8 (14)
C11—C14—C15	118.91 (18)	C24A—C27A—C26A	106.8 (18)
C11—C14—C10	60.04 (14)	C26A—C27A—C25A	96.9 (12)
N3—C17—C19	111.78 (18)		

Hydrogen-bond geometry (\AA , $^\circ$)

$D-H\cdots A$	$D-H$	$H\cdots A$	$D\cdots A$	$D-H\cdots A$
N1—H1 \cdots O4 ⁱ	0.80 (3)	2.06 (3)	2.837 (2)	165 (4)
N3—H3 \cdots O5	0.87 (3)	1.99 (3)	2.848 (4)	170 (2)
N3—H3 \cdots O5A	0.87 (3)	1.95 (3)	2.795 (10)	163 (3)
N5—H5 \cdots O2 ⁱⁱ	0.85 (3)	2.00 (3)	2.845 (2)	176 (3)
C5—H5C \cdots O2	0.98	2.51	3.119 (3)	120
C7—H7C \cdots O1 ⁱⁱⁱ	0.98	2.50	3.456 (3)	165

C12—H12A···N2	0.98	2.41	3.069 (3)	124
C24—H24C···F1 ^{iv}	0.98	2.51	3.418 (11)	154

Symmetry codes: (i) $-x+1, y+1/2, -z+1$; (ii) $-x+1, y-1/2, -z+1$; (iii) $-x+1, y-1/2, -z$; (iv) $x-1, y, z$.